

# Spatial analysis and temporal trends of daily precipitation concentration in the Mantaro River basin: central Andes of Peru

Ricardo Zubieta<sup>1,2</sup> · Miguel Saavedra<sup>1</sup> · Yamina Silva<sup>1</sup> · Lucy Giráldez<sup>1</sup>

Published online: 15 March 2016  
© Springer-Verlag Berlin Heidelberg 2016

**Abstract** The analysis of annual or seasonal data can lead to misinterpretation of spatio-temporal rainfall distribution. A high percentage of total annual precipitation can fall in just a few days, causing floods or landslides. Large economic losses from these events are particularly common in Peru, where the daily precipitation has been poorly investigated. This study presents a spatio-temporal analysis of concentration index over the Mantaro River basin in the central Peruvian Andes. Daily rainfall data recorded at 46 rainfall stations between 1974 and 2004 were selected in this study. In terms of average values, the analysis of daily rainfall indicates that low-intensity events account for 38 % of rainy days but only approximately 9 % of the total rain amount. In contrast, high- and very high-intensity events account for 35 % of rainy days and approximately 71 % of the total rain amount. The results also indicate higher concentration and lower intensity over the Northern and Central regions, compared to Southern region of the basin. Rainfall concentration gives evidence of why some of these places are more likely to be affected by extreme weather events; spatial distribution of event intensity can be partly explained by daily rainfall heterogeneity and orography. Moreover, Mann–Kendall test mostly shows a

significant change toward a weaker seasonality of daily precipitation distribution over high-mountain regions.

**Keywords** Daily precipitation · Concentration index · Peruvian Andes · Extreme events

## 1 Introduction

One of the most important aspects of climate currently requiring scientific research is the spatial and temporal variability of precipitation. Numerous studies of precipitation variability using monthly data have been carried out in the Andes using statistical techniques (Buytaert et al. 2006; Celleri et al. 2007; Silva et al. 2008; Espinoza et al. 2009; Lavado et al. 2012). Nevertheless, daily precipitation in the Andes has not been investigated to the same degree as monthly or annual precipitation (Zubieta and Saavedra 2013). In the Peruvian Andes, the rainfall analysis at daily resolution is a subject of great interest, since the presence of the Andes range contributes to a higher variability of rainfall (Espinoza et al. 2009).

Daily precipitation concentrated during a few days may increase the risks of soil erosion, landslides and floods (Coscarelli and Caloiero 2012); nonetheless, large periods without rain may also affect rain-fed agriculture. Spatio-temporal patterns of precipitation intensity are expected to change, and these extreme weather events are likely to occur more frequently (Coscarelli and Caloiero 2012). Knowledge of the spatial distribution of heavy rains is necessary for assessing the contribution of rainfall amount during rainy days, because heavy rainfall, although less frequent, contributes a large proportion of total rainfall (Suhaila and Jemain 2012). It is therefore important to analyze the statistical structure of daily precipitation. One

---

**Electronic supplementary material** The online version of this article (doi:10.1007/s00477-016-1235-5) contains supplementary material, which is available to authorized users.

---

✉ Ricardo Zubieta  
ricardo.zubieta@igp.gob.pe

<sup>1</sup> Subdirección de Ciencias de la Atmósfera e Hidrosfera (SCAH), Instituto Geofísico del Perú (IGP), Lima, Peru

<sup>2</sup> Programa de Doctorado en Recursos Hídricos, Universidad Nacional Agraria La Molina, Lima, Peru

method for describing the spatial variability of days of greatest rainfall in comparison to the total amount is the rainfall concentration index (CI) (Martin-Vide 2004). This method has been applied for statistical analysis of the occurrence of these high daily amounts, which can influence average rainfall conditions in any given month, season or year, in many places in the world, including Spain (Martin-Vide 2004), Iran (Alijani et al. 2008), China (Zhang et al. 2009), Peru (Zubieta and Saavedra 2013), Malaysia (Suhaila and Jemain 2012), Italy (Coscarelli and Caloiero 2012) and Chile (Sarricolea et al. 2013). To investigate aspects of climate change, this method also has been applied to analyze the variability in space and time of the CI in Europe (Ramos and Martinez 2006; De Luis et al. 2011; Cortesi et al. 2012; Coscarelli and Caloiero 2012) and Asia (Zhiqing et al. 2005; Shi et al. 2013a, b).

Studies in South America of daily concentration in southern and central Chile indicate higher rates for coastal plains and moderate/low rates for rainy climates on coastal range (Sarricolea et al. 2013). On the other hand, a study performed by Zubieta and Saavedra (2013) also identified irregular spatial patterns of precipitation concentrations that may be related to wind dynamics in the Andes of Peru. Such studies are particularly relevant in the Andes, where they are poorly documented. Moreover, regions such as the Mantaro River basin (MRB) in the central Andes of Peru are highly vulnerable to extreme weather events associated with climate variability; this vulnerability will increase in coming years due to climate change (IGP 2005a). The

MRB has high socioeconomic importance (1) because of the presence of hydroelectric power stations, which generate nearly 35 % of Peru's electricity, and (2) because it is the main source of agricultural products for capital, Lima (IGP 2005b). Agriculture is constantly affected by extreme rainfall events such as floods (Zubieta et al. 2012) and dry spells (Giráldez et al. 2012; Sulca et al. 2016). Additional detailed information about these extreme climatic events in this study area can be found in IGP (2012).

We hypothesize that analysis of precipitation concentration would improve knowledge of the statistical structure of daily precipitation across the Andes range. The main objectives of this paper are (1) to analyze spatial distribution of the daily rainfall concentration, (2) to determine the relationship between rainfall intensity and daily rainfall concentration, and (3) to analyze changing patterns in the concentration of daily precipitation across the study area in the central Andes of Peru.

## 2 Study area and data

The MRB is located between the Western and Eastern Ranges of the central Andes of Peru (76.65–73.9 W; 14.76–13.54S), with a drainage area of 34,550 km<sup>2</sup> (Fig. 1a) and altitudes ranging from 500 to 5300 m a.s.l., and a mean altitude of 3870 m a.s.l. (Fig. 1b). The basin is composed of glacier systems located in the Central-East part. Studies conclude that this area lost 60 % of its ice

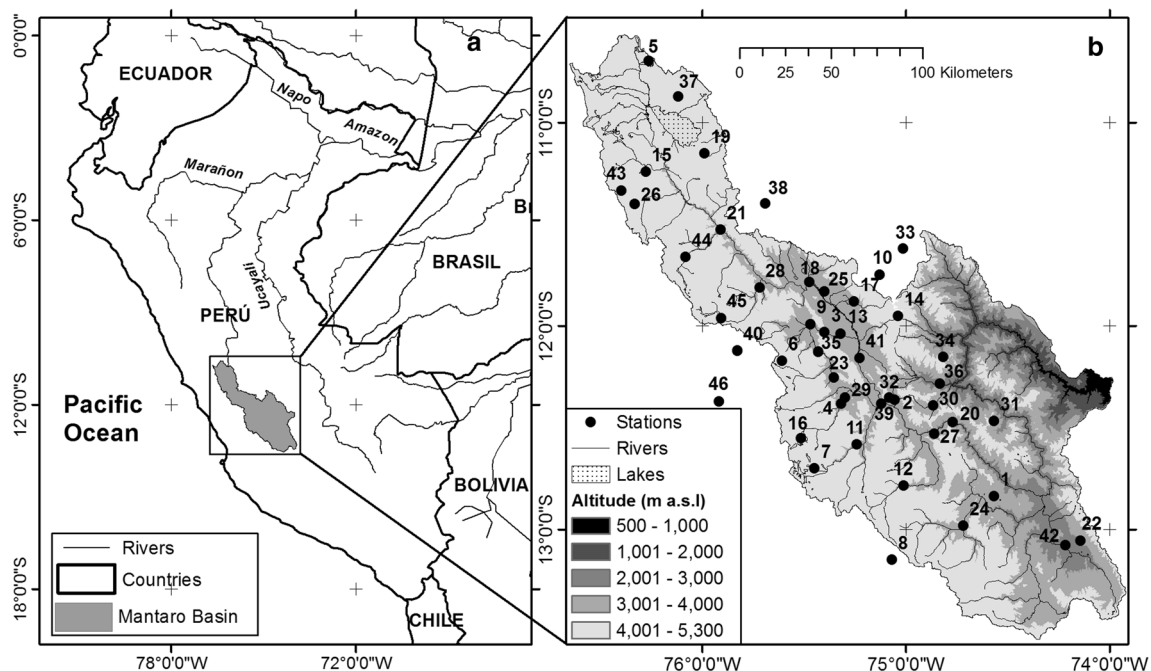


**Fig. 1** a Location of the Mantaro River basin, Peru, b the Mantaro River basin, black dots represent rainfall stations used in this work. Names of stations are indicated in Table 1

cover between 1976 and 2006 (Zubieta and Lagos 2010) and that ice cover is also associated with interannual variability of precipitation (López-Moreno et al. 2014). Average annual precipitation along the MRB is between 340 and 1300 mm/year. The largest annual precipitation (greater than 1000 mm/year) is mainly over the south-western part, while the lowest annual precipitation (less than 1000 mm/year) is in the northern and southern parts (IGP 2005a). The amplitude of the annual rainfall cycle is relatively large, with maximum values occurring between January and March and minima between June and July (Silva et al. 2008).

We collected daily rainfall data for 58 rain stations from the Instituto Geofísico del Perú (IGP), Servicio Nacional de Meteorología e Hidrología (SENAMHI), the International Research Institute (IRI) and ELECTRO-PERU (Fig. 1b; Table 1). The data period for the stations varied in duration, ranging from 13 to 48 years, between 1961 and 2011 (Table 1). Nonetheless, to ensure the highest daily data availability, we selected a common period (1974–2004) and only series with less than 5 % of missing data, this database made up of a total of 46 rain stations on a monthly basis was submitted to the regional vector method (RVM), which uses the concept of extended average rainfall to the study period to assess its quality (Hiez 1977; Brunet-Moret 1979). The least squares method is used to calculate the regional annual pluviometric index  $Z_i$ , that would have been obtained through continuous observations. This may be calculated by minimizing the sum of Eq. (1), where  $P_j$  is the extended average rainfall,  $i$  is the year index,  $j$  the station index,  $N$  the number of years, and  $M$  the number  $n$  of stations. Finally, the data series of  $Z_i$  is called regional annual pluviometric indexes vector.

$$\sum_{i=1}^N \sum_{j=1}^M \left( \frac{P_{ij}}{P_j} - Z_i \right) \quad (1)$$

Thus, a same climatic zone of the MRB, experiencing the same rainfall regime was considered, it is assumed that annual rainfall in the stations of the basin shows proportionality in between stations. Some of the observed data have also been used in the MRB for analyzing large-scale circulation associated with extreme rainfall events and their teleconnections (Sulca et al. 2016) as well as seasonal rainfall studies (Silva et al. 2008).

### 3 Methodology

To analyze spatial distribution of the daily rainfall concentration and evaluate the heaviest precipitation events, it is necessary to study the statistical structure of daily precipitation, which is adjustable by negative exponential

distributions (Jolliffe and Hope 1996). In this study, we analyzed the accumulated daily precipitation. In classifying and tabulating daily precipitation amounts in relation to rainy days, a concentration curve is obtained, where the absolute frequencies decrease exponentially, starting with the lowest class. In other words, there are many small daily amounts of precipitation and few large daily amounts (Brooks and Carruthers 1953; Martin-Vide 2004). Thus, the normalized rainfall curve obtained from this classification provides the cumulative percentage of rain amount ( $y$ ) against the cumulative percentage of rainy days ( $x$ ) (see Fig. 2a). This resultant curve obtained for each data series was fitted by an exponential curve defined in Eq. (2). The CI or irregularity of daily precipitation can be referred as a function of the relative separation between the equidistribution line (bisector) and concentration curve (area  $S'$ ) (Martin-Vide 2004).

$$y = ae^{bx} \quad (2)$$

$$CI = 2S'/10,000 \quad (3)$$

$$A' = \left[ \frac{a}{b} e^{bx} \left( x - \frac{1}{b} \right) \right]_0^{100} \quad (4)$$

To quantify the area  $S'$  enclosed by the bisector of the quadrant and the exponential curve, the Gini CI is used as a measure, as defined in Eq. (3). A definitive integral of the curve exponential between 0 and 100 is applied to calculate the area  $S'$  compressed by the curve; this area is the difference between 5000 and the value calculated from Eq. (4), where the  $a$  and  $b$  constants are determined by means of the least squares method (Martin-Vide 2004).

Thus, station Choclococha’s polygonal line represents a region with higher concentration (irregularity) of daily rainfall than that of station Huancavelica (Fig. 2b). Note that, according to station Choclococha 10 % of the rainiest days represent 35 % of the total rainfall amount (90 % of the rainy days, account for 65 % of the total), compared with 27 % for station Huancavelica (90 % of the rainy days account for 73 % of the total). A full description that Eq. (1) correspond to a valid probability distribution for daily rainfall amounts but that it is truncated when not all positive values of rainfall has non-zero probability can be found in Jolliffe and Hope (1996), and additional detailed information about the CI is also developed in Martin-Vide (2004).

To determine the relationship between rainfall intensity and daily rainfall concentration, both the average rain amount per rainy day (mm/day) (RD) and CI are calculated for comparison; these are based on the entire time interval of daily data at each rain station. A rainy day is defined as a day with rainfall of least 0.1 mm (Alijani et al. 2008). Because of there are many days with rainfall less than

**Table 1** Characteristics of rain stations in Mantaro River basin: rainy days, altitudinal location, annual mean precipitation; the station numbers correspond to those in Fig. 1b

N	Station	Rainy days	Altitude (m)	P (mm/year)	Data period (Years)
1	Acobamba	104	3236	715	1974–2004
2	Acostambo	157	3650	721	1974–2004
3	Angasmayo	104	3280	651	1974–2004
4	Cercapuquio	167	4390	855	1974–2004
5	Cerro de Pasco	187	4391	1302	1974–2004
6	Chichicocha	141	4500	771	1974–2004
7	Chilicocha	141	4200	702	1974–2004
8	Choclococha	150	4201	780	1974–2004
9	Colpa	142	3450	717	1974–2004
10	Comas	163	3300	925	1974–2004
11	Huancalpi	146	3800	915	1974–2004
12	Huancavelica	148	3676	871	1974–2004
13	Huayao	157	3308	752	1974–2004
14	Huaytapallana	190	4510	854	1974–2004
15	Hueghue	182	4175	781	1974–2004
16	Huichicocha	161	4660	683	1974–2004
17	Ingenio	133	3450	755	1974–2004
18	Jauja	138	3322	704	1974–2004
19	Junin	148	4120	859	1974–2004
20	Kichuas	130	2650	532	1974–2004
21	La Oroya	125	2651	561	1974–2004
22	La Quinua	129	3260	787	1974–2004
23	Laive	149	3990	937	1974–2004
24	Lircay	125	3150	808	1974–2004
25	Mantaro	151	3300	660	1974–2004
26	Marcapomacocha	186	4413	1149	1974–2004
27	Mejorada	143	2820	606	1974–2004
28	Pachacayo	157	3550	669	1974–2004
29	Palaco	150	3650	659	1974–2004
30	Pampas	95	3260	542	1974–2004
31	Paucarbamba	139	3000	948	1974–2004
32	Pilchaca	104	3570	728	1974–2004
33	Ricran	136	3500	655	1974–2004
34	Salcabamba	109	2900	668	1974–2004
35	San Juan de Jarpa	163	3726	1053	1974–2004
36	San Lorenzo	74	2600	542	1974–2004
37	Tambo del Sol	187	4100	866	1974–2004
38	Tarma	89	3000	340	1974–2004
39	Telleria	136	3050	566	1974–2004
40	Vilca	128	3815	826	1974–2004
41	Viques	93	3186	703	1974–2004
42	Wallapampa	89	2158	668	1974–2004
43	Yantac	165	4600	671	1974–2004
44	Yauli	209	4601	763	1974–2004
45	Yauricocha	163	4375	814	1974–2004
46	Yauyos	67	2870	478	1974–2004

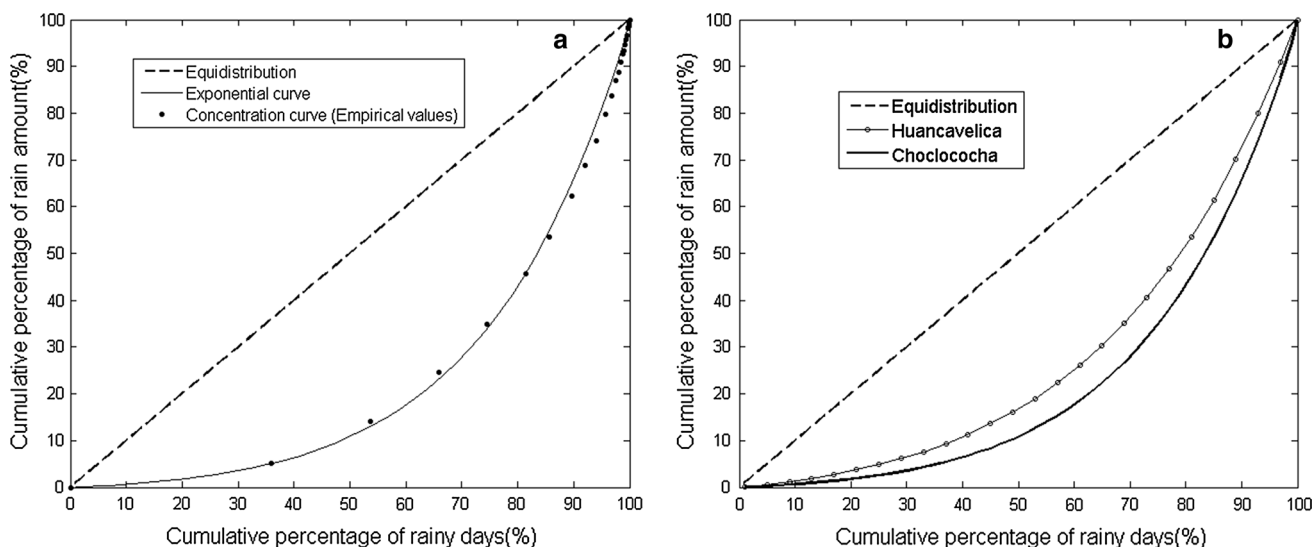


**Fig. 2** **a** Empirical values (concentration curve) and exponential curve for Choclococha station. **b** Concentration curve adjusted from exponential curve of the Huancavelica and Choclococha stations

1 mm and few days with heavy precipitation (Martin-Vide 2004).

Rainfall thresholds for the initiation of events such as landslides or floods can be variable in space and time along the MRB, in addition, extreme rainfall in one region may be normal in another. Thus, four categories according to percentiles for low-, moderate-, high- and very high-intensity events are proposed. The value of the 30th percentile is used as the rainfall threshold for a low-intensity event. Values between the 30th and 60th percentiles are considered moderate-intensity events, while values between the 60th and 80th percentiles are considered high-intensity events. Events with rainfall values recorded beyond the 80th are considered very high-intensity events. In addition, heavy rain events with values higher than the 90th percentile of cumulative rainy days are considered extreme events.

Due to the limited number of rainfall stations, the Kriging interpolation method was selected to estimate values at non-sample locations from all the appropriate inter-relationships between known and unknown values. Other Kriging methods may include algorithms called ordinary, universal, simple. Additional detailed information about these methods can be found in Isaaks and Srivastava (1989) or Lichtenstern (2013). The basic technique used in this study is the ordinary Kriging method, where a semi-variogram function is used to quantify the assumption that measurements nearby tend to be more similar than other measurements that are farther apart. The relationships between measurements are valid for a random function model and the validity of this function allow us to present equations in terms of the variogram with  $n$  locations.

$$\sum_{j=1}^n w_i Z_{ij} - \mu = Z_{i0} \quad \text{for } j = 1, \dots, n \tag{5}$$

$$\sum_{i=1}^n w_i = 1 \tag{6}$$

$$\sigma_R^2 = \sum_{i=0}^n w_i Z_{i0} + \mu \tag{7}$$

where  $Z_{ij}$  represent the semi-variances between locations  $i$  and  $j$ , and  $\mu$  is the Lagrange parameter (Eq. (5)) which is used to convert a constrained minimization problem into an unconstrained one. In this study, we use a probability model, where the optimal weight  $w_i$  are calculated such that the estimation of  $Z_{i0}$  is unbiased. To ensure unbiasedness, the sum of  $w_i$  should equal unity (Eq. (6)) with the modeled error variance  $\sigma_R^2$  given by Eq. (7). The values are weighted to derive a predicted value; their accuracy and bias were checked by cross validation (Ly et al. 2011). Cross-validation is a frequently used measure to evaluate model predictions from differences between observed and estimated values. An over-prediction or under-prediction at any point (rainfall station) can be obtained from models, thus, the mean error ME, the root mean square error RMSE and the root mean square standardized RMSS are used to evaluate them. Refer to Table S2 for more details about cross validation results.

To analyze changing patterns in concentration of daily precipitation and detect possible impacts of climatic change on precipitation time series in the central Andes of Peru, daily rainfall data from 25 rainfall stations were selected from the total (1964–2010). This period was selected because it offered the best availability spatio-



temporal of precipitation data. The CI has been calculated for each year, to detect possible trends. The temporal trend of the CI was detected by the rank-based nonparametric Mann–Kendall method (Kendall 1975; Mann 1945). This is not affected by the statistical distribution of the data and is less sensitive to outliers. Indeed, the evaluation method is based on an increase (1), decrease (−1) and equality (0) with respect to observed value. The Mann–Kendall test statistic (S) is calculated in the following Eqs. (8) and (9):

$$sgn(x_j - x_i) = \begin{cases} 1; & \text{If } x_j > x_i \\ -1; & \text{If } x_j < x_i \\ 0; & \text{If } x_j = x_i \end{cases} \quad (8)$$

$$S = \sum_{i=1}^{n-1} \sum_{j=i+1}^n sgn(x_j - x_i), \quad (9)$$

where  $sgn(x_j - x_i)$  is the sign function,  $x_i$  and  $x_j$  are the data values in time series  $i$  and  $j$  ( $j > i$ ), respectively, and  $n$  is the number of data points. The variance is computed as follows:

$$Var(S) = \frac{m(m-1)(2m+5) - \sum_{i=1}^P t_i(t_i-1)(2t_i+5)}{18}, \quad (10)$$

Where  $m$  is the number of data points,  $P$  is the number of tied groups and  $t_i$  denotes the number of ties of extent  $i$  (Eq. (10)). A tied group is a set of sample data having the same value. When  $m$  greater than 10, the standard normal test statistic  $Z_S$  is computed using Eq. (11):

$$Z_S = \begin{cases} \frac{S-1}{\sqrt{Var(S)}}, & \text{If } S > 0 \\ 0, & \text{If } S = 0 \\ \frac{S+1}{\sqrt{Var(S)}}, & \text{If } S < 0 \end{cases} \quad (11)$$

A positive  $Z$  value indicates that there is a positive trend, whereas a negative value represents a negative trend in the time series. Trend testing is done at the specific  $\alpha$  significance level, when  $|Z_S| > Z_{1-\frac{\alpha}{2}}$ , the null hypothesis is rejected and a significant trend exists in the time series.  $Z_{1-\frac{\alpha}{2}}$  is calculated from the standard normal distribution table. In this study, significance levels  $\alpha = 0.01, 0.05$  and  $\alpha = 0.10$  were used.

## 4 Results

### 4.1 General results of daily rainfall indices

The average rain amount per rainy day (RD) analyzed for all stations is 5.4 mm, with 18 % coefficient of variation (CV). This CV is slightly lower in relation to the CV calculated from the mean annual rainfall for all stations (23.7 %). The average CI calculated for the study area is 0.5, with a CV of 7 % and a low standard deviation (0.03). These statistical data would suggest a similar behavior when the daily and annual rainfall is evaluated, nonetheless, different results are obtained when low-, moderate-, high-, very high- and extreme- intensity events are analyzed.

The mean contribution of rainfall amount for extreme events is 30 % for the entire study area, and ranges from 24 to 36 % (with a CV of 9 %). This contribution occurs for approximately 9 % of the rainy days (Table 2).

The contribution of low-intensity events accounts for 36 % of the rainy days for entire MRB, representing just 9 % of total rainfall amount, with a low CV (5 %) (Table 2). These events do not suggest large environmental impacts, because of it is more likely that this rain has fallen during the dry season. The mean contribution of moderate-

**Table 2** General statistics of daily rainfall indices

Parameter	Minimum	Maximum	Mean	CV %
Averaged rainy day (RD)	0.2	53.91	5.42	18
CI	0.44	0.56	0.50	7
Extreme events (%)	24	36	30	9
Contribution of rainy days (%)				
Low intensity events	31	39	36	5
Moderate intensity events	21	30	27	6
High intensity events	17	23	19	5
Very high intensity events	17	20	18	3
Contribution of rain amount (%)				
Low intensity events	5	13	9	21
Moderate intensity events	15	23	19	11
High intensity events	22	27	24	5
Very high intensity events	42	55	48	7

Mean rain day (RD), concentration index (CI), percentages of contribution (%) for rainy days and rain amount, for low, moderate, high, very high and extreme intensity events

intensity events accounts for 27 % of the rainy days for the entire MRB, while contributing 19 % of rainfall amount. Low- and moderate-intensity events show the largest contribution of rainy days (65 %) and a low contribution of rain amount (29 %). Meanwhile, the mean contribution of high-intensity events is 19 % of rainy days and 24 % of the rain amount, and the mean contribution of very high-intensity events is 18 % of the rainy days and 48 % of the rain amount. In both high- and very high-intensity events, which are likely triggers of floods or soil erosion, there is a similarity in the contribution of rainy days (~18 %). It is important to note that those two categories contribute 37 % of the rainy days and up to 72 % of rain amount.

To investigate the relationship between daily precipitation indices and geolocation parameters, such as altitude, latitude, longitude, slope and aspect (downslope direction), correlation coefficients were calculated. The most of the indices does not show significant correlation with aspect and slope (less than 0.2), moreover, the contribution of rainy days for high- and very high-intensity events do not suggest increase with longitude ( $r = 0.2$ ), even though moisture arrives from the western part in the Amazon (Table 3). There are no significant positive or negative relationships to other events. On the other hand, the correlations between indices suggest some spatial patterns along the MRB. This is the case of RD that has positive

correlation with the contribution of rainy days for moderate-intensity events (the value of Pearson's  $r = 0.55$ ,  $p$  value  $< 0.01$ ), where the contribution of rain amount for these events also contribute to that correlation ( $r = 0.43$ ,  $p < 0.01$ ) (Table 3). This means that moderate events are more influencing on average daily rainfall for any station. Rainfall irregularity (CI) increases by contribution of rain amount due to very high-intensity and extreme events ( $r = 0.91$ ,  $p < 0.01$  and  $r = 0.84$ ,  $p < 0.01$  respectively, Table 3); this supports a high influence of these events on the calculation of CIs in relation to many environmental problems. Since the high CI uncovers regions susceptible to soil erosion, floods or landslides, in regions with predominantly low annual precipitation (Martin-Vide 2004, Coscarelli and Caloiero 2012).

#### 4.2 Spatial distribution of daily rainfall intensity and concentration index

Figure 3a shows north–south opposed regions, where the most intense rainfall (5.0–7.5 mm/day) is in the southern region, which can be mainly associated with the effect of altitude on mountain slopes, because higher intensity is seen in the southeastern, where altitudes are between 500 and 4000 m a.s.l. (see Fig. 1b). Meanwhile, less intense rainfall (3.5–5.5 mm/day) is mainly observed in the

**Table 3** Correlation coefficients of precipitation indices obtained among themselves

Contribution/parameter	RD	Rainy days contribution				CI	Rain amount contribution				Extreme
		Low	Moderate	High	Very high		Low	Moderate	High	Very high	
Lon	0.25			0.20	0.20						
Lat	-0.20										
Altitude					-0.24	0.21	-0.27		0.23		
Aspect	-0.21		-0.21			0.23		-0.29		0.23	
Slope							0.24				
RD		-0.74	<b>0.55</b>		0.62	<b>-0.45</b>	0.21	<b>0.43</b>		-0.32	
Rainy days contribution											
Low			-0.78	-0.23	-0.71	<b>0.57</b>		-0.58		0.42	
Moderate				-0.37	0.37	-0.33		<b>0.74</b>	-0.29	-0.33	
High						-0.37	0.37		<b>0.59</b>	-0.30	
Very high						-0.31			-0.38		
CI							<b>-0.89</b>	-0.74		<b>0.91</b>	
Rain amount contribution											
Low								0.50		-0.79	
Moderate										-0.83	
High										-0.25	
Very high										<b>0.96</b>	
Extreme											

Longitude (Lon), latitude (Lat), altitude, aspect, slope, mean rain day (RD), percentages of contribution (%) for rainy days and rain amount, for low, moderate, high, very high and extreme intensity events, concentration index (CI)

Bold values are significant at the 99 % level (except 0.59 which is at 95 % level)

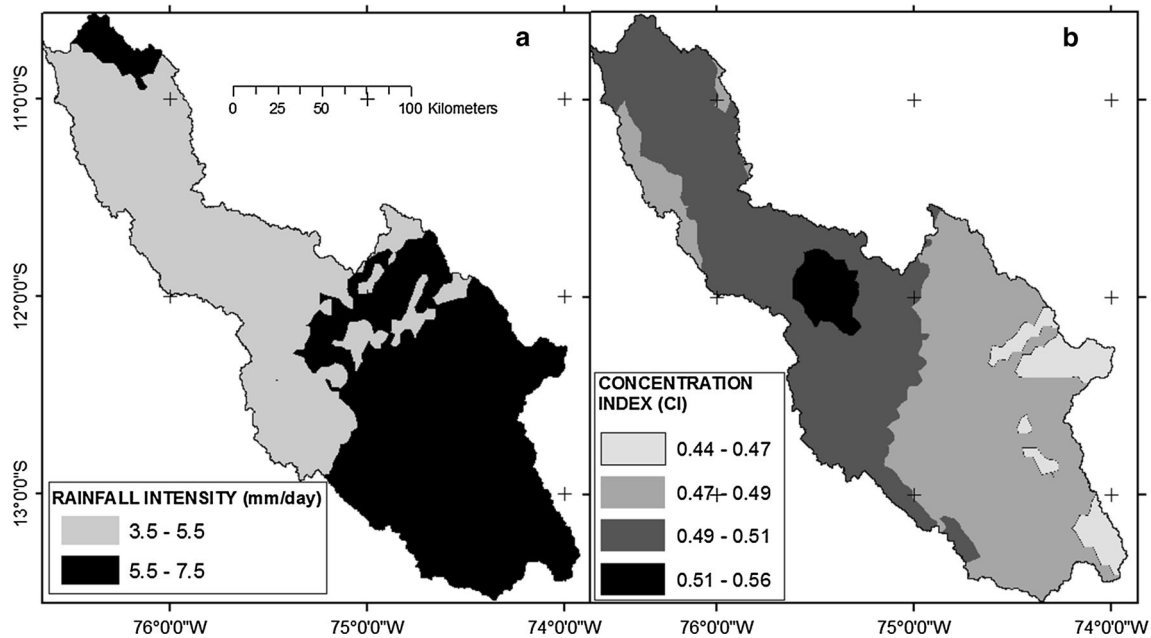


**Fig. 3** Spatial distribution of **a** average rain amount per rainy day (RD) mm/day, **b** the CI concentration index

northern region, where the threshold altitude along the western range is approximately 4000–5300 m a.s.l. This suggests an influence of orography over the arrival of moisture from the Amazon toward the MRB. Low correlation with other geolocation parameters (altitude, slope) also could be due to orography. Indeed, the South America orography is composed of different structures, one of the most important being the Andes in the western flank, which exerts individually distinct influence on the regional climate (Junquas et al. 2015).

Figure 3b shows the spatial distribution of the CI, these values range from a minimum value of 0.44 to a maximum value of 0.56. Table 4 reports the CI values for each station. In general, a value of 0.5 means that 25 % of the rainiest days contributes approximately 59 % of the total rain amount. The highest CI values (0.49–0.56) are mainly found in the northeast region, increasing toward the central region of the MRB, while in the southeast region, the majority are below the highest values (0.44–0.49). The high CI across region indicates that rainfall is more irregular; throughout the area, large or small amounts of rain could fall in a few days. These regions of the MRB is also concordant with areas such as Mantaro River valley and the Cunas, Achamayo and Shullcas River sub-basins which are frequently affected by extreme weather events that involve large economic losses and health impacts (IGP 2012).

Average annual precipitation in the northern and central regions is mainly between 340 and 900 mm/year (IGP 2005a). Nonetheless, these amounts in relation to the maximum (1300 mm/year) show that averaged annual

rainfall in the MRB conceals some aspects of rainfall irregularity, since most of this can fall in heavy precipitation events. Indeed, the spatial distribution of concentration (Fig. 3b) compared to the RD spatial distribution (Fig. 3a) does not denote direct coincidence with regions of high values. Rather, there is negative correlation ( $r = -0.45$ ,  $p < 0.01$ , Table 3).

Table 4 reports the percentage of rain contributed by 25 % of the rainiest days; these percentages range from 50.8 to 65.4 %. There is variation of 14.6 % along the MRB, reflecting a very different percentage contribution of rainy days and rain amount from site to site. It is also important to note the correlation between CI and the percentage of rain amount contributed by 25 % of the rainiest days (Table 4) is highly positive ( $r = 0.98$ ,  $p < 0.01$ ). Figure S1 shows the spatial distribution of CI for three periods. Generally, the distributions of these seasonal CI reflect a similar spatial pattern to the yearly data. Indeed, the values annual CI shows high correlation with seasonal CI during the heavy precipitation period (January–March) ( $r = 0.95$ ,  $p < 0.01$ ), dry season (May–August) ( $r = 0.91$ ,  $p < 0.01$ ) and initial rainy period (October–December) ( $r = 0.96$ ,  $p < 0.01$ ).

#### 4.3 Comparison between the CI results in Mantaro River basin and other Andean regions

The CI of the central Chile precipitation series varies between 0.53 and 0.67 mainly over coastal regions (40–1100 m a.s.l.) meanwhile, lower values are reported (0.52–0.58) over the Andes (1100–2570 m a.s.l.)



**Table 4** Values for the a and b constants of exponential curves, CI, percentage of precipitation contributed by 25 % of the rainiest days

N	Station	a	b	CI	P 25 %
1	Acobamba	0.121	0.021	0.446	53.8
2	Acostambo	0.061	0.028	0.531	62.9
3	Angasmayo	0.100	0.023	0.475	57.0
4	Cercapuquio	0.088	0.024	0.488	56.8
5	Cerro de Pasco	0.086	0.025	0.488	57.2
6	Chichicocha	0.063	0.028	0.526	61.4
7	Chilicocha	0.074	0.026	0.507	59.5
8	Choclococha	0.044	0.031	0.563	65.7
9	Colpa	0.055	0.029	0.541	63.5
10	Comas	0.099	0.023	0.473	55.9
11	Huancalpi	0.113	0.022	0.461	55.8
12	Huancavelica	0.128	0.021	0.437	50.8
13	Huayao	0.061	0.028	0.541	64.7
14	Huaytapallana	0.074	0.026	0.515	61.0
15	Hueghue	0.061	0.028	0.532	62.2
16	Huichicocha	0.080	0.025	0.498	58.0
17	Ingenio	0.068	0.027	0.524	62.2
18	Jauja	0.066	0.027	0.526	62.0
19	Junin	0.081	0.025	0.498	58.0
20	Kichuas	0.062	0.028	0.528	62.6
21	La Oroya	0.089	0.024	0.494	59.2
22	La Quinua	0.078	0.025	0.507	60.0
23	Laive	0.092	0.024	0.485	57.1
24	Lircay	0.103	0.023	0.469	55.9
25	Mantaro	0.058	0.028	0.543	64.0
26	Marcapomacocha	0.106	0.023	0.462	53.6
27	Mejorada	0.067	0.027	0.527	62.9
28	Pachacayo	0.072	0.026	0.515	61.6
29	Palaco	0.061	0.028	0.532	62.8
30	Pampas	0.122	0.021	0.446	52.7
31	Paucarbamba	0.119	0.021	0.453	54.8
32	Pilchaca	0.117	0.022	0.452	54.9
33	Ricran	0.110	0.022	0.463	54.6
34	Salcabamba	0.116	0.021	0.458	54.3
35	San Juan de Jarpa	0.082	0.025	0.494	57.6
36	San Lorenzo	0.114	0.022	0.458	55.2
37	Tambo del Sol	0.069	0.027	0.519	61.1
38	Tarma	0.125	0.021	0.449	55.0
39	Telleria	0.063	0.028	0.531	63.0
40	Vilca	0.094	0.024	0.480	56.2
41	Viques	0.063	0.028	0.527	61.7
42	Wallapampa	0.123	0.021	0.441	52.8
43	Yantac	0.105	0.022	0.468	55.4
44	Yauli	0.106	0.022	0.472	56.5
45	Yauricocha	0.075	0.026	0.504	58.5
46	Yauyos	0.096	0.023	0.478	56.6

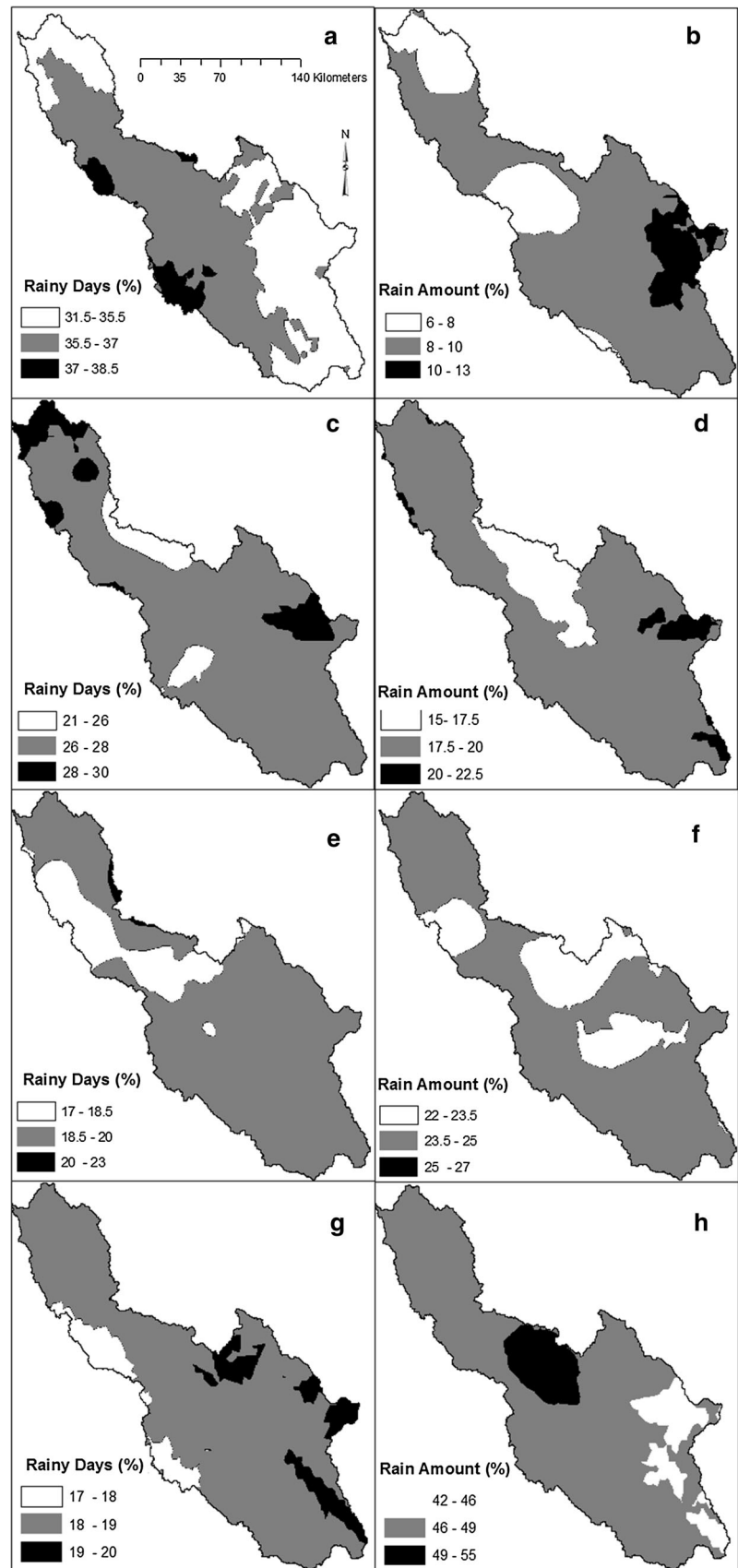
(Sarricolea et al. 2013). Nevertheless, CI values estimated in this study (0.44–0.56) on the MRB (500–5300 m a.s.l.) in the Peruvian Andes are lower, thus, the percentage of rain amount contributed by 25 % of the rainiest days is also lower (Table 4). The result may due to the different climatic systems of the central part of Chile (32.83–34.2°S) which is mainly characterized by semiarid conditions with annual precipitation lower than 350 mm (Rutllant and Fuenzalida 1991). Sarricolea et al. (2013) showed that the spatial distribution of the CI values are associated to the seasonal variations of subtropical precipitation and the special topography of the region, with the coast to the west and the Andes to the east, represents an orographic control. Indeed, the Andes range in this region acts as an effective barrier isolating the region from the Atlantic influence (Montecinos and Aceituno 2003). The most of rainfall in central part of Chile is originated by cold fronts associated with migratory low pressure systems embedded in the midlatitude westerlies (Saavedra et al. 2002; Montecinos et al. 2000). On the other hand, the onset of the South American Monsoon System (SAMS) and warming of the continent are related to rainfall seasonality in the region of the Peruvian Andes, as water vapor can enter the Amazon basin the in austral summer and to its demise in winter (Zhou and Lau 1998). These features also influence the uplift of moisture from the Amazon towards the upper Andes due to the coupling of the Andes with the upper level Bolivian High and easterly winds (Garreaud 1999).

#### 4.4 Spatial distribution of rainfall events

To analyze the spatial distribution of rainy days and rain amount contributions, two maps representing each event category have been produced (Fig. 4). Figure 4a, b shows the spatial distribution for low-intensity events. The two maps have different spatial patterns, showing that their contributions differ greatly. A large percentage of rainy days, ranging from 31 to 39 %, contribute up to just 13 % of the total rain amount. Their highest percentages of rainy day contributions are in the northern and central regions (Fig. 4a), which show a pattern similar to that of the CI distribution (Fig. 3b) ( $r = 0.57$ ,  $p < 0.01$ ), in contrast, rain amount is negatively correlated with CI ( $r = -0.89$ ,  $p < 0.01$ ) (Table 3).

The rainy day and rain amount contributions for moderate-intensity events (Fig. 4c, d) show similar spatial patterns between them. Correlation value between the two contributions is 0.74 (significant at the 99 % level) (Table 3). These events contribute more to rainfall than low-intensity events (see Fig. 4b–d), rainy days range from

**Fig. 4** Percentage contribution of rainy days and rain amount for intensity events: **a, b** low, **c, d** moderate, **e, f** high and **g, h** very high



21 to 30 % and contribute between 15 and 23 % of total rainfall.

The spatial distribution of contribution for high-intensity events is mapped in Fig. 4e, f, which shows that these events represent 17–23 % of rainy days and contribute between 22 and 27 % of total rain. As with moderate-intensity events, there is significant correlation between rainy days and rain amount for high-intensity events ( $r = 0.59$ ,  $p < 0.05$ ) (Table 3). Similar spatial patterns across the MRB can be also seen in both maps, where the greatest contributions appear over the northern and southern region. These patterns between rainy days and rain amount when moderate- and high-intensity events are analyzed, could be due to a marked seasonality of rainfall, because of these events are more probably developed during initial rainy (October–December) and heavy precipitation periods (January–March).

Andes regions are exposed to extreme weather and climate events, such as unusually intense precipitation, causing high erosion rates, which is associated to climate variability (Pepin et al. 2013; Lowman and Barros 2014). The contribution percentages for very high-intensity events are mapped in Fig. 4g, h, which shows that rainy days of between 17 and 20 % contribute up to 55 % of total rain. This category of intensity contributes a larger amount of rain than the others, and the amount of rain associated with these events is highly correlated with CI ( $r = 0.96$ ,  $p < 0.01$ ) (Table 3). Rainy days for very high-intensity events are more frequent in the eastern part of the basin, but the highest values for rain amount contribution are found in central region. This central region also shows a high contribution of rain amount for extreme events, up to 35 % (Fig. 5), as well as a high correlation with CI ( $r = 0.84$ ,  $p < 0.01$ ). These findings show that rainfall irregularity is mainly associated with high- and very high-intensity events in the northern and central regions of the MRB, where there is also environmental risk from extreme rainfall.

#### 4.5 Trends in daily precipitation concentration

To detect possible trends, in this paper the precipitation CI has been estimated for each year. It should be noted that the majority of the CI precipitation series do not show a significant trend. Nevertheless, more series show a positive trend than a negative trend for the three periods analyzed (January–March, May–August and October–December) (Fig. 6).

For the heavy precipitation period (January–March), the number of rain stations with positive CI trends is much higher than those with negative trends (10-3). The positive CI trends are mainly concentrated in the western and northeastern parts of the MRB. Of 25 rainfall stations, four

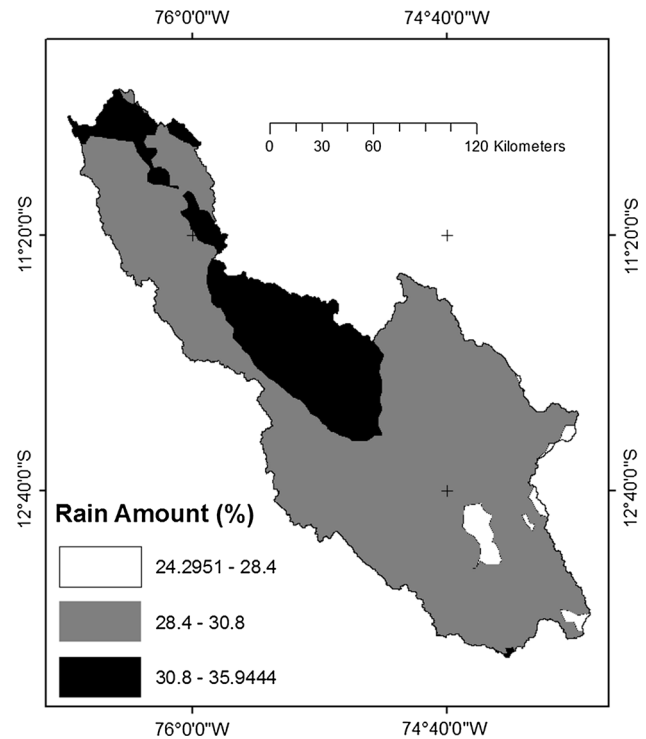


**Fig. 5** Percentage contribution of rain amount for extreme events

rainfall series show a trend at significance level between 90 and 95 %, one shows a trend at significance level between 95 and 99 %, and five show a significant trend at significance level greater than 99 %. For the dry season (May–August), the number of rain stations with positive CI trends is greater than those with negative trends (6-3). As with the heavy precipitation period, these positive CI trends are also located in the western and northeastern parts of the MRB, where four of the rainfall series show a significant trend at significance level between 90 and 95 % and two series show a significant trend at significance level between 95 and 99 %. As with the dry season, for the initial rainy period (October–December), the number of rain stations with positive CI trends is also slightly higher than those with negative trends (4-3), and the positive CI trends are located in the same regions of the MRB. Four of these rainfall series show a significant trend at significance level greater than 99 %. These positive trends of CI differs the results of IGP (2005c), which estimated a negative trend for the heavy precipitation period (especially, in January and March) (Stations: Huayao, Junin, Tambo de Sol, Cerro de Pasco, San Juan de Jarpa) from monthly time series. In general, increased CI contributes to a high impact on environmental phenomena, such as floods, soil erosion or long periods without rain, which complicates good management of water resources.

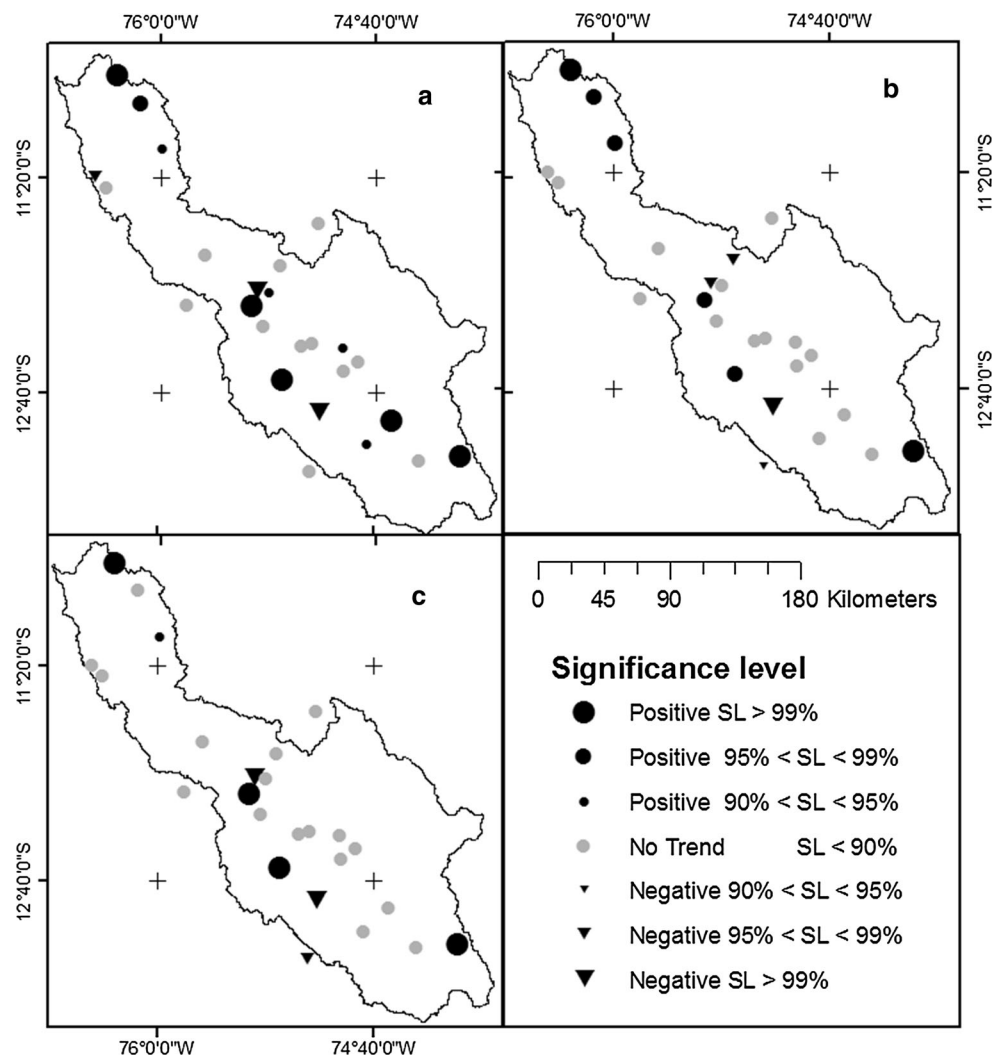


**Fig. 6** Seasonal CI trend distributions (1964–2010) in the Mantaro River basin for different ranges of the significance level (SL): **a** January–March, **b** May–August, **c** October–December. Positive trends are *black circles* and negatives are *black triangles*; *gray circle* does not present trends

## 5 Discussion and conclusions

Most of the rainfall information analyzed in Peru is based on annual, seasonal or monthly data that nonetheless is derived from daily time series. In this paper, daily rainfall data were used to study the spatial distribution of rainfall concentration over the Mantaro River basin in the central Andes of Peru. Results from analysis of a daily rainfall CI indicate that large amounts of annual rainfall can occur in just a few days. To analyze daily rainfall concentration, the categories of low-, moderate-, high-, very high- and extreme-intensity events were proposed. The analysis indicates that low-intensity events account for an average of 36 % of rainy days, contributing approximately 9 % of the total rain amount. In contrast, high- and very high-intensity events account for 35 % of rainy day contribution

and approximately 71 % of the rain amount. Our results show that rain amount contribution is highly related to daily rain concentration for extreme-intensity events. The maximum concentration of daily rainfall indicates why some regions are more likely to be affected by flash floods or landslides. The differences and similarities between concentration and intensity of daily rainfall suggest an influence of orography on the arrival of moisture from the Amazon toward the upper Andes.

The computed concentration index of CI values ranges between 0.44 and 0.56 in the Mantaro River basin, smaller than CI values of 0.53–0.67 in the central region of Chile (Sarricolea et al. 2013) and much smaller than others mountains regions (0.50–0.80) such as the Lancang River basin of south central China (Shi et al. 2013b) likely due to the different climatic systems. The Mantaro River basin is

influenced by the onset of the South American Monsoon System and warming of the continent towards the upper Andes, they are related to tropical rainfall seasonality, making daily precipitation relatively less irregular than other regions. Comparatively, climate conditions in central region of Chile are controlled by subtropical cold fronts from the midlatitude westerlies. Meanwhile, Lancang River basin is characterized by subtropical monsoon climate from the Bay of Bengal that favors large amounts of rainfall.

Precipitation concentration trends were analyzed using the Mann–Kendall test; seasonal CI (January–March, May–August, and October–December) was also calculated for each year. This shows that daily precipitation has clear tendency to decrease the amplitude of seasonal cycle of rainfall, and suggests higher impacts on the environment. These results may help better water resources management and prevent the underestimation of risks from floods or soil erosion, during heavy precipitation period, since they result in large economic losses in the basin.

The reliable quantification of the spatio-temporal distribution of rainfall is fundamental for analyzing extreme climatic events in real or quasi-real time. Satellites are an alternative source of rainfall data and its use would allow to know the spatio-temporal distribution of the CI over high mountain regions, where ground-based measurement networks (meteorological or hydrological) can be scarce or nonexistent. Indeed, it is necessary to evaluate the usefulness of these datasets in daily rainfall concentration studies; as analyzed similarly in hydrological studies on the Andes range (Zubieta et al. 2015). To that end, the first Global Precipitation Measurement (GPM) observations and Tropical Rainfall Measuring Mission (TRMM) product 3B42 should be tested in relation to ground-based precipitation.

**Acknowledgments** The authors would like to thank the Instituto Geofísico del Perú (IGP), Servicio Nacional de Meteorología e Hidrología (SENAMHI), International Research Institute (IRI) and ELECTRO-PERU for providing observed data; and J. Chunga for their support in data preprocessing. The first author thanks suggestions and comments raised during the MAREMEX project (IGP), which was supported by the International Development Research Centre: IDRC-Canada. Suggestions from D. Ramirez and A. Verastegui and B. Fraser were greatly appreciated.

## References

- Alijani B, O'Brien J, Yarnal B (2008) Spatial analysis of precipitation intensity and concentration in Iran. *Theor Appl Climatol* 94:107–124. doi:10.1007/s00704-007-0344-y
- Brooks CEP, Carruthers N (1953) *Handbook of statistical methods in meteorology*. Meteorological Office, London
- Brunet-Moret Y (1979) Homogénéisation des précipitations. *Cahiers ORSTOM Sér Hydrol* 16:3–4
- Buytaert W, Celleri R, Willems P (2006) Spatial and temporal rainfall variability in mountainous areas: a case study from the south Ecuadorian Andes. *J Hydrol* 329:413–421. doi:10.1016/j.jhydrol.2006.02.031. ISSN:0022-1694
- Celleri R, Willems P, Buytaert W, Feyen J (2007) Space–time rainfall variability in the Paute basin, Ecuadorian Andes. *Hydrol Process* 21:3316–3327. doi:10.1002/hyp.6575
- Cortesi N, Gonzalez-Hidalgo JC, Brunetti M, Martin-Vide J (2012) Daily precipitation concentration across Europe 1971–2010. *Nat Hazards Earth Syst Sci* 12:2799–2810. doi:10.5194/nhess-12-2799-2012
- Coscarelli R, Caloiero T (2012) Analysis of daily and monthly rainfall concentration in Southern Italy (Calabria region). *J Hydrol* 416–417:145–156. doi:10.1016/j.jhydrol.2011.11.047
- De Luis M, Gonzalez-Hidalgo JC, Brunetti M, Longares LA (2011) Precipitation concentration changes in Spain 1946–2005. *Nat Hazards Earth Syst Sci* 11:1259–1265. doi:10.5194/nhess-11-1259-2011
- Espinoza JC, Ronchail J, Guyot JL, Cocheneau G, Filizola N, Lavado W, de Oliveira E, Pombosa R, Vauchel P (2009) Spatio-temporal rainfall variability in the Amazon Basin Countries (Brazil, Peru, Bolivia, Colombia and Ecuador). *Int J Climatol* 29:1574–1594. doi:10.1002/joc.1791
- Garreaud RD (1999) Multiscale analysis of the summertime precipitation over the central Andes. *Mon Weather Rev* 127(5):901–921
- Giráldez L, Silva Y, Trasmonte G (2012) Impacto de los veranillos en la agricultura del valle del Mantaro. *Libro Manejo de riesgos de desastres ante eventos meteorológicos extremos en el valle del Mantaro, Volumen II. Resultados del proyecto MAREMEX*. Instituto Geofísico del Perú, Lima
- Hiez G (1977) L'homogénéité des données pluviométriques. *Cahiers ORSTOM Sér Hydrol* 14:129–172
- IGP (2005a) Vulnerabilidad actual y futura ante el cambio climático y medidas de adaptación en la Cuenca del Río Mantaro. Fondo Editorial del CONAM, Lima
- IGP (2005b) Diagnóstico de la cuenca del río Mantaro bajo la visión de cambio climático. Fondo Editorial CONAM, Lima
- IGP (2005c) Atlas Climatológico de precipitaciones y temperaturas en la Cuenca del Mantaro. Fondo Editorial CONAM, Lima
- IGP (2012) Manejo de riesgos de desastres ante eventos meteorológicos extremos en el valle delMantaro, Volumen II. Resultados del proyecto MAREMEX. Instituto Geofísico del Perú, Lima
- Isaaks EH, Srivastava RM (1989) *An introduction to applied geostatistics*. Oxford University Press, New York
- Jolliffe IT, Hope PB (1996) Representation of daily rainfall distributions using normalized rainfall curves. *Int J Climatol* 16:1157–1163
- Junquas C, Li L, Vera CS, Le Treut H, Takahashi K (2015) Influence of South America orography on summer time precipitation in Southeastern South America. *Clim Dyn*. doi:10.1007/s00382-015-2814-8
- Kendall MG (1975) *Rank correlation methods*. Griffin, London
- Lavado WC, Labat D, Ronchail J, Espinoza JC, Guyot JL (2012) Trends in rainfall and temperature in the Peruvian Amazon-Andes basin over the last 40 years (1965–2007). *Hydrol Process* 27:2944–2957. doi:10.1002/hyp.9418
- Lichtenstern A (2013) *Kriging methods in spatial statistics*, Bachelor's Thesis, Department of Mathematics, Technische Universität München
- López-Moreno I, Fontaneda S, Bazo J, Revuelto J, Azorin-Molina C, Valero-Garcés B, Morán-Tejeda E, Vicente-Serrano SM, Zubieta R, Alejo-Cochachín J (2014) Recent glacier retreat and climate



- trends in Cordillera Huaytapallana, Peru. *Glob Planet Change* 112(2014):1–11. doi:[10.1016/j.gloplacha.2013.10.010](https://doi.org/10.1016/j.gloplacha.2013.10.010)
- Lowman LEL, Barros AP (2014) Investigating links between climate and orography in the central Andes: coupling erosion and precipitation using a physical-statistical model. *J Geophys Res Earth Surf* 119:1322–1353. doi:[10.1002/2013JF002940](https://doi.org/10.1002/2013JF002940)
- Ly S, Charles C, Degré A (2011) Geostatistical interpolation of daily rainfall at catchment scale: the use of several variogram models in the Ourthe and Ambleve catchments, Belgium. *Hydrol Earth Syst Sci* 15:2259–2274. doi:[10.5194/hess-15-2259-2011](https://doi.org/10.5194/hess-15-2259-2011)
- Mann HB (1945) Nonparametric tests against trend. *Econometrica* 13:245–259
- Martin-Vide J (2004) Spatial distribution of a daily precipitation concentration index in Peninsular Spain. *Int J Climatol* 24:959–971. doi:[10.1002/joc.1030](https://doi.org/10.1002/joc.1030)
- Montecinos A, Aceituno P (2003) Seasonality of the ENSO-related rainfall variability in central Chile and associated circulation anomalies. *J Clim* 16:281–296. doi:[10.1175/1520-0442\(2003\)016<0281:SOTERR>2.0.CO;2](https://doi.org/10.1175/1520-0442(2003)016<0281:SOTERR>2.0.CO;2)
- Montecinos A, Díaz A, Aceituno P (2000) Seasonal diagnostic and predictability of rainfall in subtropical South America based on tropical Pacific SST. *J Clim* 13:746–758. doi:[10.1175/1520-0442\(2000\)013<0746:SDAPOR>2.0.CO;2](https://doi.org/10.1175/1520-0442(2000)013<0746:SDAPOR>2.0.CO;2)
- Pepin E, Guyot J, Armijos E, Bazan H, Fraizy P, Moquet JS, Noriega L, Lavado W, Pombosa R, Vauchel P (2013) Climatic control on eastern Andean denudation rates (Central Cordillera from Ecuador to Bolivia). *J S Am Earth Sci* 44:85–93. doi:[10.1016/j.jsames.2012.12.010](https://doi.org/10.1016/j.jsames.2012.12.010)
- Ramos MC, Martínez JA (2006) Trends in precipitation concentration and extremes in the Mediterranean Penedès—Anoia Region, NE Spain. *Clim Change* 74:457–474. doi:[10.1007/s10584-006-3458-9](https://doi.org/10.1007/s10584-006-3458-9)
- Rutllant J, Fuenzalida H (1991) Synoptic aspects of the central Chile rainfall variability associated with the Southern Oscillation. *Int J Climatol* 11:63–76. doi:[10.1002/joc.3370110105](https://doi.org/10.1002/joc.3370110105)
- Saavedra N, Müller EP, Foppiano AJ (2002) Monthly mean rainfall frequency model for the Central Chile coast: some climatic inferences. *Int J Climatol* 22:1495–1509. doi:[10.1002/joc.806](https://doi.org/10.1002/joc.806)
- Sarricolea P, Herrera MJ, Araya C (2013) Análisis de la concentración diaria de las precipitaciones en Chile central y su relación con la componente zonal (subtropicalidad) y meridiana (orográfica). *Investig Geogr Chile* 45:37–50
- Shi P, Qiao X, Chen X, Zhou M, Qu S, Ma X, Zhang Z (2013a) Spatial distribution and temporal trends in daily and monthly precipitation concentration indices in the upper reaches of the Huai River, China. *Stoch Environ Res Risk Assess*. doi:[10.1007/s00477-013-0740-z](https://doi.org/10.1007/s00477-013-0740-z)
- Shi W, Yu X, Liao W, Wang Y, Jia B (2013b) Spatial and temporal variability of daily precipitation concentration in the Lancang River basin. *J Hydrol*. doi:[10.1016/j.jhydrol.2013.05.002](https://doi.org/10.1016/j.jhydrol.2013.05.002)
- Silva Y, Takahashi K, Chávez R (2008) Dry and wet rainy seasons in the Mantaro river basin (Central Peruvian Andes). *Adv Geosci* 14:261–264. doi:[10.5194/adgeo-14-261-2008](https://doi.org/10.5194/adgeo-14-261-2008)
- Suhaila J, Jemain AA (2012) Spatial analysis of daily rainfall intensity and concentration index in Peninsular Malaysia. *Theor Appl Climatol* 108:235–245. doi:[10.1007/s00704-011-0529-2](https://doi.org/10.1007/s00704-011-0529-2)
- Sulca J, Vuille M, Silva Y, Takahashi K (2016) Teleconnections between the Peruvian Central Andes and Northeast Brazil during extreme rainfall events in Austral summer. *J Hydrometeorol* 17:499–515. doi:[10.1175/JHM-D-15-0034.1](https://doi.org/10.1175/JHM-D-15-0034.1)
- Zhang Q, Xu CY, Gemmer M, Chen YQ, Liu CL (2009) Changing properties of precipitation concentration in the Pearl River basin, China. *Stoch Environ Res Risk Assess* 23:377–385. doi:[10.1007/s00477-008-0225-7](https://doi.org/10.1007/s00477-008-0225-7)
- Zhiqing X, Yin D, Aijun J, Yuguo D (2005) Climatic trends of different intensity heavy precipitation events concentration in China. *J Geogr Sci* 15(4):459–466. doi:[10.1360/gso50409](https://doi.org/10.1360/gso50409)
- Zhou J, Lau KM (1998) Does a monsoon climate exist over South America? *J Clim* 11:1020–1040. doi:[10.1175/1520-0442\(1998\)011<1020:DAMCEO>2.0.CO;2](https://doi.org/10.1175/1520-0442(1998)011<1020:DAMCEO>2.0.CO;2)
- Zubieta R, Lagos P (2010) Cambios de la superficie glaciar en la cordillera Huaytapallana: Periodo 1976–2006. Libro Cambio climático en la cuenca del río Mantaro. Balance de 7 años de estudio en la cuenca del Mantaro. Instituto Geofísico del Perú
- Zubieta R, Saavedra M (2013) Distribución espacial del índice de concentración de precipitación diaria en los Andes centrales peruanos: valle del río Mantaro. *Revista del Encuentro Científico Internacional ECI Peru* 9(2):61–70
- Zubieta R, Quijano J, Latínez K, Guillermo P (2012) Evaluación de las zonas de peligro frente a inundaciones por máximas avenidas en el valle del río Mantaro. Manejo de riesgos de desastres ante eventos meteorológicos extremos en el valle del Mantaro, vol II. Proyecto Maremex Mantaro. Instituto Geofísico del Perú, Lima
- Zubieta R, Geritana A, Espinoza JC, Lavado W (2015) Impacts of satellite-based precipitation datasets on rainfall-runoff modeling of the western Amazon basin of Peru and Ecuador. *J Hydrol*. doi:[10.1016/j.jhydrol.2015.06.064](https://doi.org/10.1016/j.jhydrol.2015.06.064)